A comparison of methods for a priori bias correction in soil moisture data assimilation

Sujay V. Kumar,[1,2] Rolf H. Reichle,[3] Kenneth W. Harrison,[2,4] Christa D. Peters-Lidard,[2] Soni Yatheendradas,[2,4] and Joseph A. Santanello[2]

Received 18 November 2010; revised 3 February 2012; accepted 6 February 2012; published 13 March 2012.

[1] Data assimilation is increasingly being used to merge remotely sensed land surface variables such as soil moisture, snow, and skin temperature with estimates from land models. Its success, however, depends on unbiased model predictions and unbiased observations. Here a suite of continental-scale, synthetic soil moisture assimilation experiments is used to compare two approaches that address typical biases in soil moisture prior to data assimilation: (1) parameter estimation to calibrate the land model to the climatology of the soil moisture observations and (2) scaling of the observations to the model's soil moisture climatology. To enable this research, an optimization infrastructure was added to the NASA Land Information System (LIS) that includes gradient-based optimization methods and global, heuristic search algorithms. The land model calibration eliminates the bias but does not necessarily result in more realistic model parameters. Nevertheless, the experiments confirm that model calibration yields assimilation estimates of surface and root zone soil moisture that are as skillful as those obtained through scaling of the observations to the model's climatology. Analysis of innovation diagnostics underlines the importance of addressing bias in soil moisture assimilation and confirms that both approaches adequately address the issue.

Citation: Kumar, S. V., R. H. Reichle, K. W. Harrison, C. D. Peters-Lidard, S. Yatheendradas, and J. A. Santanello (2012), A comparison of methods for a priori bias correction in soil moisture data assimilation, *Water Resour. Res.*, *48*, W03515, doi:10.1029/2010WR010261.

1. Introduction

[2] Land data assimilation systems merge satellite or in situ observations of land surface fields (such as soil moisture, snow and skin temperature) with estimates from land surface models. Observations are often discontinuous in space and time, and their incorporation into the modeled estimates helps generate spatially complete and temporally continuous estimates of land surface fields. The process of combining observations and model forecasts is typically carried out by weighting each on the basis of their respective errors. The uncertainty in model states results from model structural deficiencies, errors in model parameter specifications and input forcings. Similarly, observational data also suffer from errors caused by instrument noise and errors associated with the retrieval models. A key assumption in most data assimilation techniques is that the errors in observations and model forecasts are strictly random and that on average, the observations and model estimates agree with the true estimates. In reality, however, biases are unavoidable and it is difficult to attribute the bias to the model or the observations. Nevertheless, the proper treatment of such systematic errors is critical for the success of data assimilation systems [*Dee and da Silva*, 1998].

[3] A number of prior studies have described techniques to address the treatment of bias errors in data assimilation systems. *Dee* [2005] characterizes the data assimilation systems as either "bias blind" or "bias aware" on the basis of their treatment of systematic errors. The bias-blind systems are designed to correct random, zero-mean errors and assume the use of unbiased observations relative to the model-generated background. For soil moisture, the absolute levels of continental-scale estimates from land surface models and satellite observations differ significantly [*Reichle et al.*, 2004, 2007], which implies a need for "bias-aware" approaches to soil moisture assimilation. An often used method to address such biases is to rescale the observations prior to data assimilation in such a way that the observational climatology matches that of the land model [*Reichle and Koster*, 2004; *Drusch et al.*, 2005; *Crow et al.*, 2005; *Slater and Clark*, 2006; *Reichle et al.*, 2007; *Draper et al.*, 2009; *Kumar et al.*, 2009; *Reichle et al.*, 2010; *Liu et al.*, 2011; *Draper et al.*, 2011]. Put differently, these so-called a priori scaling approaches assimilate normalized deviates or percentiles instead of the raw observations. A priori scaling is easy to implement as a preprocessing step to the data assimilation system and does not make assumptions about whether the climatology of

[1]Science Applications International Corporation, Beltsville, Maryland, USA.
[2]Hydrological Sciences Laboratory, NASA Goddard Space Flight Center, Greenbelt, Maryland, USA.
[3]Global Modeling and Assimilation Office, NASA Goddard Space Flight Center, Greenbelt, Maryland, USA.
[4]Earth System Science Interdisciplinary Center, College Park, Maryland, USA.

Copyright 2012 by the American Geophysical Union
0043-1397/12/2010WR010261

the model or that of the observations is more correct. Although the resulting analyses are produced in the model's climatology, they can be scaled back to the observational climatology, if needed. However, since the computation of the climatologies is conducted as a preprocessing step, the corrections cannot easily be adjusted to dynamic changes in bias.

[4] Dynamically bias-aware assimilation systems, on the other hand, incorporate specific assumptions about the nature of biases and are specifically built to estimate and correct them. These strategies typically attribute the bias to either the model or the observations and use the analysis increments in the data assimilation system to estimate the bias. Variants of such dynamic bias correction strategies have been used in soil moisture assimilation studies [*De Lannoy et al.*, 2007a, 2007b] and for land surface temperature assimilation by *Bosilovich et al.* [2007] and *Reichle et al.* [2010]. In these studies, the observations are assumed to be unbiased, and the bias is attributed to model exclusively. In reality, however, the retrievals from different sensors may be biased against each other [*Reichle et al.*, 2007; *Trigo and Viterbo*, 2003]. The key advantage of the dynamic bias estimation and correction approaches is their ability to adapt to transient changes in bias.

[5] In this paper, we explore an alternative strategy for a priori bias correction that has not been used for continental-scale soil moisture assimilation: the a priori calibration of land surface model (LSM) parameters. We use optimization algorithms to estimate model parameters that minimize the bias between model forecasts and observations. Similar to the a priori scaling methods discussed above, the a priori calibration approach complements the state update steps of the data assimilation system. In the latter, the model forecast is modified only when observations are present. In the absence of observational information, the model will revert back to its original climatology. Adjusting model parameters offers a way to bring the model's climatology in line with that of the observations, including at times and locations where observations are intermittently absent. Like a priori scaling, a priori model calibration does not adjust dynamically to changes in model or observation bias.

[6] Model parameters have long been recognized as a key source of errors in model predictions, and many LSM studies have focused on the application of techniques to estimate them [*Duan et al.*, 1992; *Burke et al.*, 1997; *Gupta et al.*, 1999; *Hogue et al.*, 2005; *Liu et al.*, 2004, 2005; *Santanello et al.*, 2007; *Peters-Lidard et al.*, 2008; *Lambot et al.*, 2009; *Gutman and Small*, 2010; *Nearing et al.*, 2010]. These studies estimate LSM parameters using independent observations of variables such as soil moisture, streamflow and surface temperature. In addition, data assimilation studies have also recognized the need to update and estimate model parameters for improving the model's predictive skills. A number of studies have examined the potential of parameter estimation in conjunction with state estimation in sequential data assimilation systems [*Boulet et al.*, 2002; *Moradkhani et al.*, 2005a, 2005b; *Qin et al.*, 2009; *Yang et al.*, 2009; *Nie et al.*, 2011; *Montzka et al.*, 2011; *DeChant and Moradkhani*, 2011]. These approaches, known as joint estimation or state augmentation methods, estimate the model parameters concurrently with the model states. Such approaches, however, have difficulties in handling the relative time invariance of parameters (compared to model states) and very large parameter spaces [*Liu and Gupta*, 2007]. *De Lannoy et al.* [2007a] note that in some situations it may be better to estimate the bias separately rather than correct it using state augmentation methods. An approach that employs the simultaneous use of optimization and data assimilation was described by *Vrugt et al.* [2005], where the model parameters are estimated through the recursive calibration over a data assimilation instance. This method considers the estimation of model parameter sets for generating the best possible forecasts, when model states are also adjusted through sequential data assimilation. The advantages and limitations of these joint state and parameter estimation approaches are discussed in detail by *Liu and Gupta* [2007].

[7] Here we compare, in the context of data assimilation, the approach of bias mitigation through the estimation of model parameters against a priori bias correction strategies that rescale the observations to conform to the model's climatology. The parameter estimation is performed in a "batch calibration" mode, where a set of observational data is used to estimate time-invariant model parameters with the objective of minimizing the climatological differences between the model and the observations. The model with the calibrated parameters is subsequently employed in the data assimilation system to assimilate the raw, unscaled observations. In contrast, the scaling approaches essentially assimilate the anomaly information instead of the raw observations. We investigate these methods with a soil moisture assimilation case study. A new generation of satellite soil moisture retrievals are becoming available from the recently launched Soil Moisture and Ocean Salinity (SMOS) [*Kerr et al.*, 2010] and the planned Soil Moisture Active Passive (SMAP) [*Entekhabi et al.*, 2010b] missions. The results from our study are directly relevant to the effective utilization of these new observations in land data assimilation systems.

[8] The experiments presented in this paper are conducted using the NASA Land Information System (LIS) [*Kumar et al.*, 2006; *Peters-Lidard et al.*, 2007], which is a multiscale modeling system for hydrologic applications developed with the goal of integrating satellite- and ground-based observational data products and advanced land surface models and techniques to generate improved estimates of land surface conditions. LIS includes a suite of subsystems to support land surface modeling for a variety of applications, including a comprehensive sequential data assimilation system, based on the NASA Global Modeling and Assimilation Office's infrastructure [*Reichle et al.*, 2009; *Kumar et al.*, 2008b]. More recently, a generic optimization subsystem has been developed within LIS, with the goal of combining the use of optimization and data assimilation in an integrated framework. This new extension to LIS will be described in detail below and was used to facilitate the experiments discussed here.

[9] The paper is organized as follows. The design and capabilities of the optimization subsystem within LIS are presented first (section 2). This is followed by the description of the experiment setup that evaluates the use of parameter estimation in data assimilation (section 3). The results from the data assimilation integrations are presented

in section 4. Finally, section 5 discusses the conclusions from the study.

2. Optimization Subsystem in LIS

[10] LIS is designed as an object-oriented framework, where all functional extensions (such as land surface models, data assimilation algorithms, meteorological inputs, observational data, etc.) are implemented as abstract, extensible components [*Kumar et al.*, 2006, 2008a]. A large suite of modeling extensions have been incorporated in LIS using this design paradigm. The optimization subsystem in LIS is designed in a similar interoperable manner.

2.1. Optimization Abstractions

[11] Generically, an optimization instance can be stated as a problem of determining unknown parameters by minimizing or maximizing an objective function subject to a number of constraints. The optimization subsystem in LIS defines three functional abstractions on the basis of this generic form, shown in Figure 1: (1) objective function, (2) decision/parameter space, and (3) algorithm used to solve the optimization problem. In the instance of parameter estimation, the decision space is defined by the list of LSM parameters (or a subset thereof). The objective function object represents the function or criteria to be maximized or minimized. Examples include the minimization of squared residuals and the maximization of likelihood measures. Finally, the optimization algorithm abstraction represents the actual search strategy used to find the optimal solution. The interconnections between these three generic pieces are handled within the LIS core, which is the unit that enables the integrated use of various extensible components in LIS. Custom implementations of each of these three abstractions constitute a specific instance of an optimization problem.

[12] Similar to the design of the LIS data assimilation subsystem [*Kumar et al.*, 2008b], the data exchanges between these abstractions are handled through the constructs of the Earth System Modeling Framework (ESMF) [*Hill et al.*, 2004]. ESMF provides a standardized, self-describing format for data exchange between these components. Three search algorithms of varying complexity are implemented in this infrastructure: (1) Levenberg-Marquardt (LM) [*Levenberg*, 1944; *Marquardt*, 1963], (2) shuffled complex evolution from the University of Arizona (SCE-UA) [*Duan et al.*, 1992, 1993], and (3) genetic algorithm (GA) [*Holland*, 1975]. LM is a gradient-based search technique and is suited only for deterministic convex optimization problems, whereas SCE-UA and GA are more suited for difficult combinatorial optimization problems such as LSM parameter estimation.

2.2. Genetic Algorithm

[13] In this article, we employ GA for estimating LSM parameters. GAs are stochastic search techniques that use heuristics-based principles of natural evolution and genetics. The algorithm works by employing a population of individuals (or candidate solutions), each of which is represented by a set of values of the problem's variables that need to be estimated (also called decision space). By applying operations that are based on natural evolution concepts, such as selection, recombination and mutation, the population evolves toward better solutions over several generations (or iterations).

[14] Figure 2 depicts a flowchart showing the sequence of GA operations during optimization. A fitness value that reflects the quality of the solution and its ability to satisfy constraints and objectives of the problem is associated with each potential solution. The selection operator simulates the "survival of the fittest" behavior by preferentially selecting the solutions with higher fitnesses to be present in the subsequent populations. As a result, solutions with good traits survive and solutions with bad traits are eliminated. Each pair of selected solutions then undergoes the recombination step where two new solutions are generated

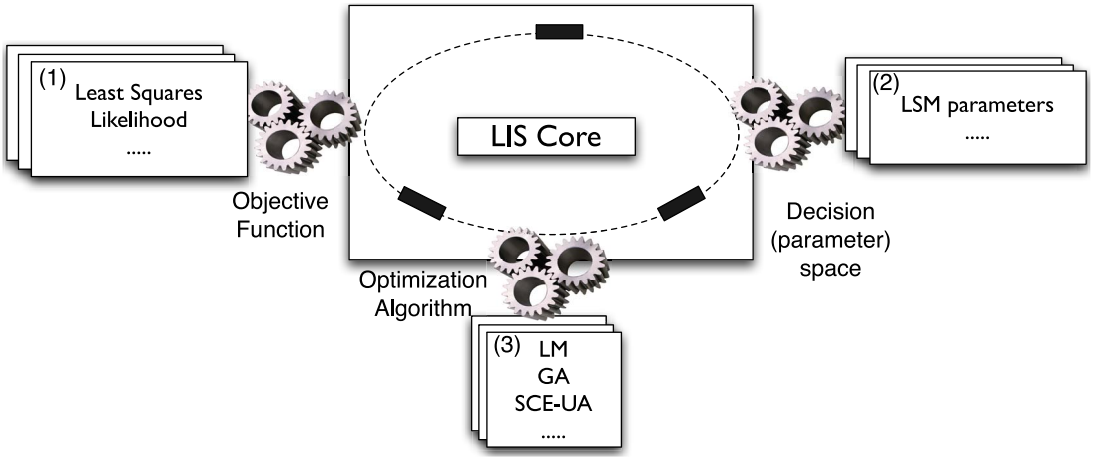

Figure 1. Optimization abstractions in the NASA Land Information System (LIS): (1) objective function, (2) decision/parameter space, and (3) optimization algorithm (LM, Levenberg-Marquardt; GA, genetic algorithm; SCE-UA, shuffled complex evolution from the University of Arizona). Dotted lines represent interconnections between the optimization abstractions enabled by the LIS core. Black boxes represent data exchanges between the three components through the Earth System Modeling Framework (ESMF) objects.

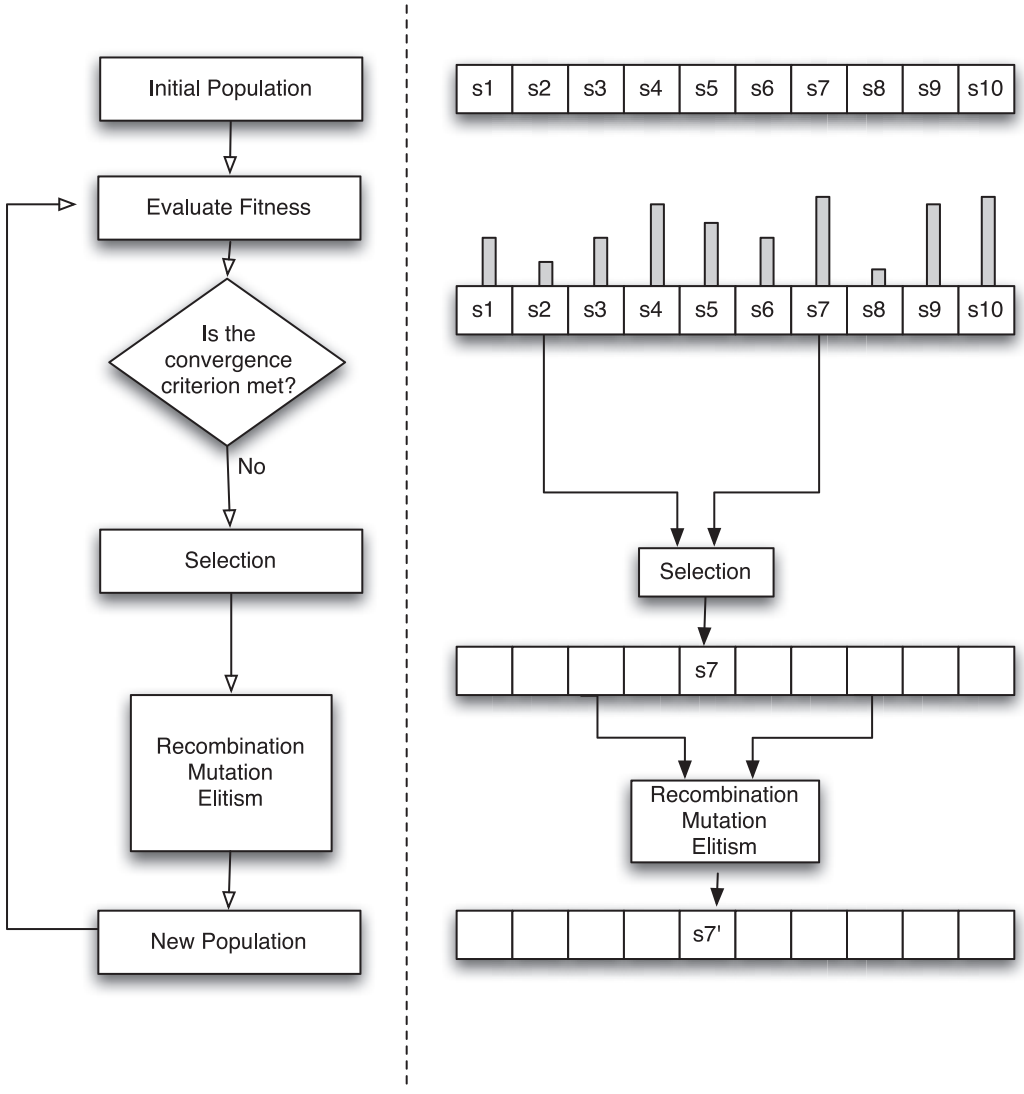

Figure 2. Sequence of GA operations. An example of the population evolution is shown on the right, with a population size of 10 potential solutions (s1, s2, . . . , s10). The gray bars indicate the fitness values of the individual solutions. An example of the selection step shows the choice of s7 after comparing s2 and s7. After the selection step, the GA operations of recombination, mutation, and elitism are conducted, and a new population of solutions is generated. The algorithm continues until the convergence criteria are met.

by combining the "genes" of the parent solutions. The mutation operator is used to infuse the population with gene values that may not be present in the population. The recombination and mutation rates define the probability of crossover between any two pairs and the probability of a gene undergoing mutation, respectively. To ensure that the best solution in any generation is not lost through these probabilistic recombination and mutation operations, a strategy named elitism is used. Elitism ensures that the best solution from the previous generation is compared with the worst solution in the current generation, replacing the current generation's solution, if better. These steps are repeated through several iterations (or generations) until the specified convergence criteria is met.

[15] GAs do not rely upon local or gradient information and are able to deal with complexities in the search space such as the presence of local optima and discontinuities. GAs are also well suited to handle discrete decision variables and nonlinearity in the simulation models effectively. The problem-independent structure of the algorithm has enabled its application in many areas of science and engineering [*Goldberg*, 1989]. GAs, however, require the evaluation of several simulation runs to obtain the best solution, making them computationally intensive. The high-performance computing tools in LIS are employed for mitigating this limitation (section 4.3).

3. Experimental Setup

3.1. Experiment Overview

[16] In section 3.1, we describe a suite of synthetic data assimilation experiments that examines parameter estimation as an a priori bias mitigation scheme. In addition, two variants of the a priori scaling method are used:

standard-normal deviate scaling [*Crow et al.*, 2005] and cumulative distribution function (CDF) matching [*Reichle and Koster*, 2004]. The experiment setup is similar to that of *Kumar et al.* [2009], but only two land surface models are used here. The Noah land surface model (version 2.7.1 [*Ek et al.*, 2003]) employs the four-layer soil model of *Mahrt and Pan* [1984] with thicknesses (listed from top to bottom) of 10, 30, 60, and 100 cm. In the catchment LSM [*Koster et al.*, 2000], the vertical soil moisture profile is determined through deviations from the equilibrium soil moisture profile between the surface and the water table. Soil moisture in the 0–2 cm surface layer and in the 0–100 cm root zone layer is diagnosed from the modeled soil moisture profile. The catchment LSM typically employs hydrologically defined catchments (or watersheds) as basic computational units. In this study, however, the catchment LSM is used on a regular latitude-longitude grid to facilitate the model intercomparison.

[17] Using these land surface models, we conducted a suite of synthetic "fraternal twin" assimilation experiments. The basic structure of the experiments is as follows: First, a soil moisture simulation is conducted with the catchment LSM to generate the assumed "true" state of the land surface, referred to as the control (or "truth") run. Second, the observations to be assimilated are generated from this truth run by introducing realistic retrieval errors. Third, a suite of data assimilation integrations are conducted by assimilating these synthetic observations into the Noah land surface model, using different bias mitigation strategies. The Noah model integration without any data assimilation is referred to as the "open loop" simulation. The assimilation integrations are conducted using a one-dimensional ensemble Kalman filter (EnKF) algorithm (see *Reichle and Koster* [2003] for details on 1D versus 3D filtering). The performance of the assimilation approaches is evaluated by comparing against the known true fields (from the catchment LSM integration).

3.2. Experiment Details

[18] All model simulations are conducted on a gridded domain that roughly covers the continental United States (CONUS, from 30.5°N, 124.5°W to 50.5°N, 75.5°W) at 1° spatial resolution, using a 30 min model time step. Surface meteorological boundary conditions from the Global Data Assimilation System (GDAS; the global meteorological weather forecast model of the National Centers for Environmental Prediction [*Derber et al.*, 1991]) are used to drive the LSMs. The models are cycled three times through the period from 1 January 2000 to 1 January 2006 to ensure that internal model states are in equilibrium with the forcing meteorology and parameters. The initial conditions generated from this "spin-up" process are used in the data assimilation and open loop integrations except those that use the optimized parameters. The optimization-based integrations use the soil moisture initial conditions estimated through calibration (section 3.3). All model and assimilation integrations are conducted over the above mentioned 6 year period.

[19] Each open loop or assimilation experiment with the Noah LSM consists of 12 ensemble members [*Kumar et al.*, 2008b], and the mean of the ensemble is used in the evaluations. In order to maintain an ensemble of model fields representing the uncertainty in soil moisture, perturbations are applied to select meteorological and model prognostic fields. The parameters used for these perturbations are based on previous work [*Reichle et al.*, 2007; *Kumar et al.*, 2009] and are listed in Table 1. Zero-mean, normally distributed additive perturbations are applied to the downward longwave radiation forcing, and lognormal multiplicative perturbations with a mean value of 1 are applied to the precipitation and downward shortwave fields (Table 1). Time series correlations are imposed via a first-order regressive model (AR(1)) with a time scale of 24 h. No spatial correlations are applied since this study uses the one-dimensional version of the EnKF. Cross correlations are imposed on the perturbations of radiation and precipitation fields using the values specified in Table 1.

[20] In addition to the forcing perturbations, the Noah model prognostic variables for soil moisture are perturbed with additive noise that is vertically correlated (Table 1). For the perturbations to the model prognostics we impose AR(1) time series correlations with a 12 h time scale. The perturbation settings do not introduce systematic biases in the open loop integrations relative to a standard, unperturbed, single-member model integration (not shown).

[21] A set of preprocessing steps are applied to the synthetic retrievals generated from the catchment LSM integration. To account for difficulties in retrieving soil moisture products from microwave sensors, the synthetic observations are masked out when the green vegetation

Table 1. Parameters for Perturbations to Meteorological Forcings and Model Prognostic Variables in the Ensemble Kalman Filter Assimilation Experiments

Variable	Perturbation Type	Standard Deviation	Cross Correlations With Perturbations						
			SW ↓	LW ↓	PCP	sm1	sm2	sm3	sm4
Meteorological Forcings									
Downward shortwave (SW ↓)	multiplicative	0.3	1.0	−0.5	−0.8				
Downward longwave (LW ↓)	additive	50 W m^{-2}	−0.5	1.0	0.5				
Precipitation (PCP)	multiplicative	0.50	−0.8	0.5	1.0				
Noah LSM Soil Moisture States									
Total soil moisture									
Layer 1 (sm1)	additive	6.0E-3 m^3 m^{-3}				1.0	0.6	0.4	0.2
Layer 2 (sm2)	additive	1.1E-4 m^3 m^{-3}				0.6	1.0	0.6	0.4
Layer 3 (sm3)	additive	0.60E-5 m^3 m^{-3}				0.4	0.6	1.0	0.6
Layer 4 (sm4)	additive	0.40E-5 m^3 m^{-3}				0.2	0.4	0.6	1.0

fraction values exceed 0.7 and when snow or precipitation are present. Random Gaussian noise with an error standard deviation of 0.03 m^3 m^{-3} (volumetric soil moisture) is added to the catchment model surface soil moisture values to mimic measurement uncertainties. This error standard deviation is chosen as an estimate of the expected error level in surface soil moisture retrievals from upcoming spaceborne L band radiometers [*Kerr et al.*, 2010; *Entekhabi et al.*, 2010b].

[22] Five different data assimilation integrations are conducted using these synthetic observations (Table 2): DA-NOSC, using unscaled observations without any bias correction, DA-STDN, using a priori scaled observations based on standard normal deviate scaling, DA-CDF, using a priori scaled observations based on CDF matching, DA-OPT1, using unscaled observations with a calibrated model, where the model parameters were estimated using a single year of batch calibration (year 2000), and DA-OPT6, using unscaled observations with a calibrated model, where model parameters were optimized using all 6 years (2000–2006) of observations.

[23] The approaches that employ a priori scaling of observations (DA-STDN and DA-CDF) represent the commonly followed approaches of correcting biases prior to data assimilation by scaling the observations into the model climatology. The DA-CDF experiment follows the strategy of *Reichle and Koster* [2004] and matches the CDF of the observations to that of the model soil moisture. First, the observation and model CDFs are computed independently for each grid cell using the 6 year period. Next, the observations are rescaled, separately for each grid cell, such that their climatology matches that of the model soil moisture. In theory, this approach corrects all moments of the distribution regardless of its shape, although in practice the correction of higher-order moments is naturally limited by the sample size. While the climatological differences between the model and the observations may change with season [*Drusch et al.*, 2005], our experiment DA-CDF is based on CDFs derived with data from all seasons lumped together as done by *Reichle et al.* [2007]. The standard normal deviate-based scaling used in the DA-STDN experiment is a simpler approach that matches only the first and second moments of the observation and model distributions but breaks the scaling down by calendar month to account for possible seasonal changes in the climatological differences. This approach is used, for example, by *Crow et al.* [2005]). For a given calendar month k and a given grid cell i, the scaling parameters are the multiyear mean ($\overline{\theta}^m_{i,k}$ and $\overline{\theta}^o_{i,k}$ for model and observations, respectively) and multiyear standard deviation ($\sigma^m_{i,k}$ and $\sigma^o_{i,k}$ for model and observations, respectively). For all observations θ_i from this particular calendar month (time subscript omitted), the scaled observations θ'_i are then given by

$$\theta'_i = \overline{\theta}^m_{i,k} + (\theta_i - \overline{\theta}^o_{i,k})\frac{\sigma^m_{i,k}}{\sigma^o_{i,k}} \tag{1}$$

[24] In contrast, the calibration-based integrations (DA-OPT1 and DA-OPT6) assimilate raw (unscaled) observations and rely on the calibrated model parameters to mitigate bias in the data assimilation system. Note that in the four experiments with bias correction, the information from the observation set is employed twice. In DA-STDN and DA-CDF, the observations are used once for deriving the climatology and then for assimilation, when the scaled observations are assimilated. Similarly, in DA-OPT1 and DA-OPT6, the same set of observations is employed twice, once for the calibration of the model climatology and then again for the subsequent data assimilation. We do not separate the periods of model calibration and data assimilation in experiments DA-OPT1 and DA-OPT6 in order to provide an equivalent comparison to DA-STDN and DA-CDF.

[25] Note that a priori scaling and model calibration are intended to address the relative bias between the model and the observations. The data assimilation system then works with a set of observations that are unbiased relative to the model background. In this sense, the synthetic experiment used here represents the issues in a "real" data assimilation system. The long-term mean and variability of satellite, in situ, and model soil moisture estimates differ from each other because of representativeness differences (horizontal and vertical), limited sensor calibration, retrieval model assumptions, and model deficiencies, implying that, in a climatological sense, none of the data sets is necessarily more correct than any other [*Reichle and Koster*, 2004; *Reichle et al.*, 2007]. Consequently, our use of the truth label for the synthetic observations does not necessarily imply that satellite-based retrievals are unbiased.

3.3. Optimization Formulation for Parameter Estimation

[26] In experiments DA-NOSC, DA-STDN, and DA-CDF we use the Noah LSM with its native parameters that are mostly based on look-up tables (as functions of vegetation and soil categories), the same parameters that are used

Table 2. Overview of Model and Assimilation Integrations

Model	Description
OL	Noah model integration without assimilation (open loop)
OPT1	Noah model integration without assimilation and with model parameters optimized to reproduce 1 year (2000) climatology of synthetic soil moisture observations
OPT6	Noah model integration without assimilation and with model parameters optimized to reproduce 6 years (2000–2006) climatology of synthetic soil moisture observations
DA-NOSC	Noah assimilation integration without bias correction using unscaled observations
DA-STDN	Noah assimilation integration using a priori scaling of observations based on standard normal deviates
DA-CDF	Noah assimilation integration using a priori scaling of observations based on cumulative distribution function (CDF) matching
DA-OPT1	Noah assimilation integration using OPT1 model parameters and unscaled observations
DA-OPT6	Noah assimilation integration using OPT6 model parameters and unscaled observations

in the operational environments at the National Centers for Environmental Prediction (NCEP) and the Air Force Weather Agency (AFWA). For experiments DA-OPT1 and DA-OPT6, by contrast, we estimate spatially distributed representations of Noah model parameters through GA optimization (section 4.1).

[27] Table 3 lists the parameters included in the decision space in the optimization simulations based on the work by *Hogue et al.* [2005]. The decision space includes a number of vegetation and soil properties along with the initial soil moisture states. The initial set of potential solutions in GA is generated by randomly sampling from the range of each parameter as specified in Table 3. A population size of 50 is used in the GA simulations.

[28] The objective function at each grid point is defined as the inverse of absolute difference in the mean soil moisture values of the observation and the model (equation (2)), where J_i is the fitness value for grid cell i and $\overline{\theta}_i^o$ and $\overline{\theta}_i^m$ are the mean soil moisture values from the observations (from catchment LSM) and simulated from Noah model, respectively, for grid cell i. The mean soil moisture values $\overline{\theta}_i^o$ and $\overline{\theta}_i^m$ are computed at each grid point i by averaging the available soil moisture values over the course of the model simulation. The denominator of the objective function thus represents the absolute soil moisture climatology difference between the observations and the model.

$$J_i = \left(\frac{1}{|(\overline{\theta}_i^o - \overline{\theta}_i^m)|} \right) \tag{2}$$

This objective function is maximized independently for each grid cell i. The optimization explores the decision space to maximize the fitness function values, subject to the allowed range of values for each parameter (Table 3).

[29] The GA integrations use an elitism strategy to ensure that the current best solution is not overwritten during GA evolution. A mutation rate of 0.005 and a recombination rate of 0.9 was employed. The algorithm was found to converge after approximately 200 generations, when the fitness of the best solution was found not to improve in the last 30 generations. These GA parameters (including the mutation and recombination rates) are chosen largely from experience and the success of the optimization simulations presented in section 4.1 suggest that they are reasonable.

4. Results

[30] The results presented in section 4 focus first on the optimization simulations, that is, the model calibration conducted prior to the DA-OPT1 and DA-OPT6 assimilation integrations. Following this discussion, the different bias mitigation strategies are evaluated within the context of soil moisture data assimilation.

4.1. Optimization Simulations

[31] Two separate optimization simulations are conducted: (1) using a single year of observational data (OPT1; observations from year 2000) and (2) using observations from all 6 years (OPT6; years 2000–2006). First, we compare the Noah model integrations using these two sets of LSM parameters with the open loop simulation that

Table 3. List of Noah Land Surface Model Parameters Used in the Optimization Runs[a]

Variable	Description	Minimum Value	Maximum Value
smcmax	porosity	0.30	0.55
psisat	saturated matric potential	0.01	0.70
dksat	saturated hydraulic conductivity (m s^{-1})	0.05E-5	3.00E-5
dwsat	saturated soil diffusivity	5.71E-6	2.33E-5
bexp	the "b" parameter	3.0	9.0
quartz	soil quartz content	0.10	0.90
rsmin	minimum stomatal resistance (m)	40	1000
rgl	parameter used in solar radiation term of canopy resistance	30	150
hs	parameter used in vapor pressure deficit term of canopy resistance	36.35	55
z0	roughness length (m)	0.01	0.99
lai	leaf area index	0.05	6.00
cfactr	canopy water parameter	0.1	2.0
cmcmax	canopy water parameter (m)	1E-4	2E-3
sbeta	parameter used in the computation of vegetation effect on soil heat flux	−4	−1
rsmax	maximum stomatal resistance (m)	2000	10,000
topt	optimum transpiration air temperature (K)	293	303
refdk	reference value for saturated hydraulic conductivity (m s^{-1})	5E-7	3E-5
fxexp	bare soil evaporation exponent	0.2	4.0
refkdt	reference value for surface infiltration parameter	0.1	10.0
czil	parameter used in the calculation of roughness length of heat	0.05	0.8
csoil	soil heat capacity for mineral soil component	1.26E6	3.5E6
frzk	ice threshold	0.10	0.25
snup	snow depth threshold that implies 100% snow cover (m)	0.02	0.08
sh2o1	initial liquid soil moisture for soil layer 1 (m^3 m^{-3})	0.05	0.50
sh2o2	initial liquid soil moisture for soil layer 2 (m^3 m^{-3})	0.05	0.50
sh2o3	initial liquid soil moisture for soil layer 3 (m^3 m^{-3})	0.05	0.50
sh2o4	initial liquid soil moisture for soil layer 4 (m^3 m^{-3})	0.05	0.50
smc1	initial total soil moisture for soil layer 1 (m^3 m^{-3})	0.05	0.50
smc2	initial total soil moisture for soil layer 2 (m^3 m^{-3})	0.05	0.50
smc3	initial total soil moisture for soil layer 3 (m^3 m^{-3})	0.05	0.50
smc4	initial total soil moisture for soil layer 4 (m^3 m^{-3})	0.05	0.50

[a]The columns show the variable names, a brief description, and the range of values (maximum and minimum values) of the parameters used in the optimization system.

employs the default values from the look-up table. Figure 3 presents maps of time series mean (climatological) differences in surface soil moisture (which is essentially the inverse of the objective function used in the optimization simulations). As discussed in section 3.3, the maps are computed by subtracting the mean Noah LSM soil moisture values for each of the integrations shown in Figure 3 from the corresponding mean catchment LSM surface soil moisture estimates. In computing these mean fields, we only include the times and locations for which (synthetic) observations are available (section 3.2). Further, only grid points with at least 600 observations for the evaluation period are considered in the analysis of the results.

[32] Figure 3 demonstrates that using the optimized parameters leads to reducing the systematic differences in climatologies between the model and observations, throughout the domain. These maps indicate that the Noah open loop integration generates on average (but not uniformly) drier soil moisture values compared to the catchment LSM. The use of optimized parameters helps to correct the bias. Both OPT1 and OPT6 integrations improve this systematic underestimation in the open loop by providing closer matches to the catchment (truth) estimates, as seen in Figures 3b and 3c. The domain-averaged soil moisture climatology difference is reduced from 0.034 m^3 m^{-3} (for OL) to 0.006 m^3 m^{-3} for OPT1 and to −0.003 m^3 m^{-3} for OPT6. If absolute values of climatology differences are used, the improvements from OPT1 and OPT6 are even more pronounced; the domain-averaged absolute difference reduces from 0.047 m^3 m^{-3} for OL to 0.010 m^3 m^{-3} for OPT1 and 0.009 m^3 m^{-3} for OPT6. The estimation of model parameters thus enables the correction of systematic biases and leads to a closer match between the soil moisture climatologies of the model (Noah) and the synthetic observations (catchment).

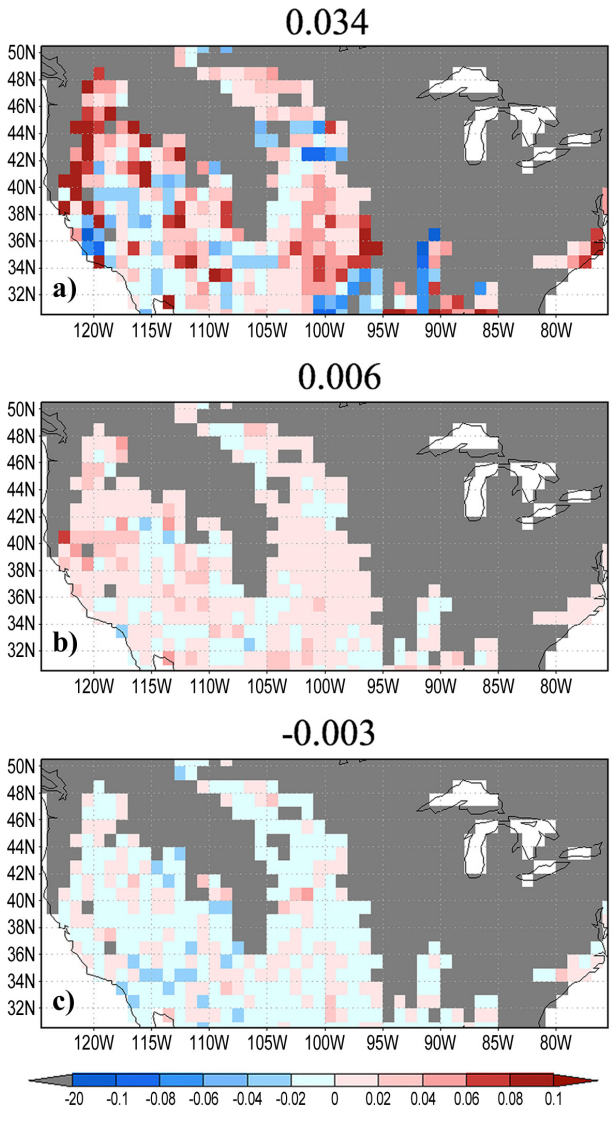

Figure 3. Comparison of the surface soil moisture climatology difference fields between the catchment LSM truth and (a) OL (b) OPT1, and (c) OPT6 (see Table 2). The gray color represents grid cells excluded from the computations. Titles indicate domain-averaged values. The units are m^3 m^{-3}.

[33] Figure 4 shows maps of the parameters used in the open loop integration (prescribed using look-up tables) and the calibrated values from the OPT6 integration. Out of the parameters listed in Table 3 we focus on three key parameters: porosity (θ_s), saturated matric potential (ψ_s) and saturated hydraulic conductivity (K_s). The spatial patterns in the look-up table–based parameters are similar to each other, because they are determined on the basis of the soil texture map. In contrast, the optimized parameters show more spatial variability because they are not constrained to soil types or vegetation categories. Compared to the default parameters, the optimized parameters in general show higher values of θ_s, ψ_s, and K_s over the domain. This is consistent with the optimization objective of correcting the dry bias in the open loop integration, as higher values of θ_s, ψ_s, and K_s would allow for more water to be held in the soil and more infiltration into the soil, and correspondingly higher soil moisture values. Similar spatial trends are also observed in other parameters (not shown).

[34] Although these spatial trends are consistent with the patterns in soil moisture simulations, the intent here is not to judge the veracity or physical realism of the estimated parameters. Instead, our goal is to study how bias mitigation through parameter estimation helps in the subsequent data assimilation performance. Though the typical approach in land surface models is to employ look-up table–based parameters that are derived from limited data samples [e.g., *Rawls et al.*, 1982; *Cosby et al.*, 1984], these representations suffer from numerous issues, including lack of spatial representativeness of the data sets on which they are based, errors in extrapolating the point-scale to the modeling scales, and the large within–soil class variation of properties that is on par with the variation across different texture classes [*Schaap*, 2004; *Braun and Schadler*, 2005; *Doherty and Welter*, 2010; *Gutman and Small*, 2010]. Further, the physical realism and mismatch issues of the parameters are difficult to assess at large spatial scales because validating in situ measurements of surface and root zone soil moisture that match the scale of the model grid cells are not available.

[35] In short, there is significant uncertainty associated with the default parameters, typically regarded as the truth. The optimization formulation in this article samples from the ranges of parameters (Table 3) representing the full spectrum across all look-up table categories. Additional

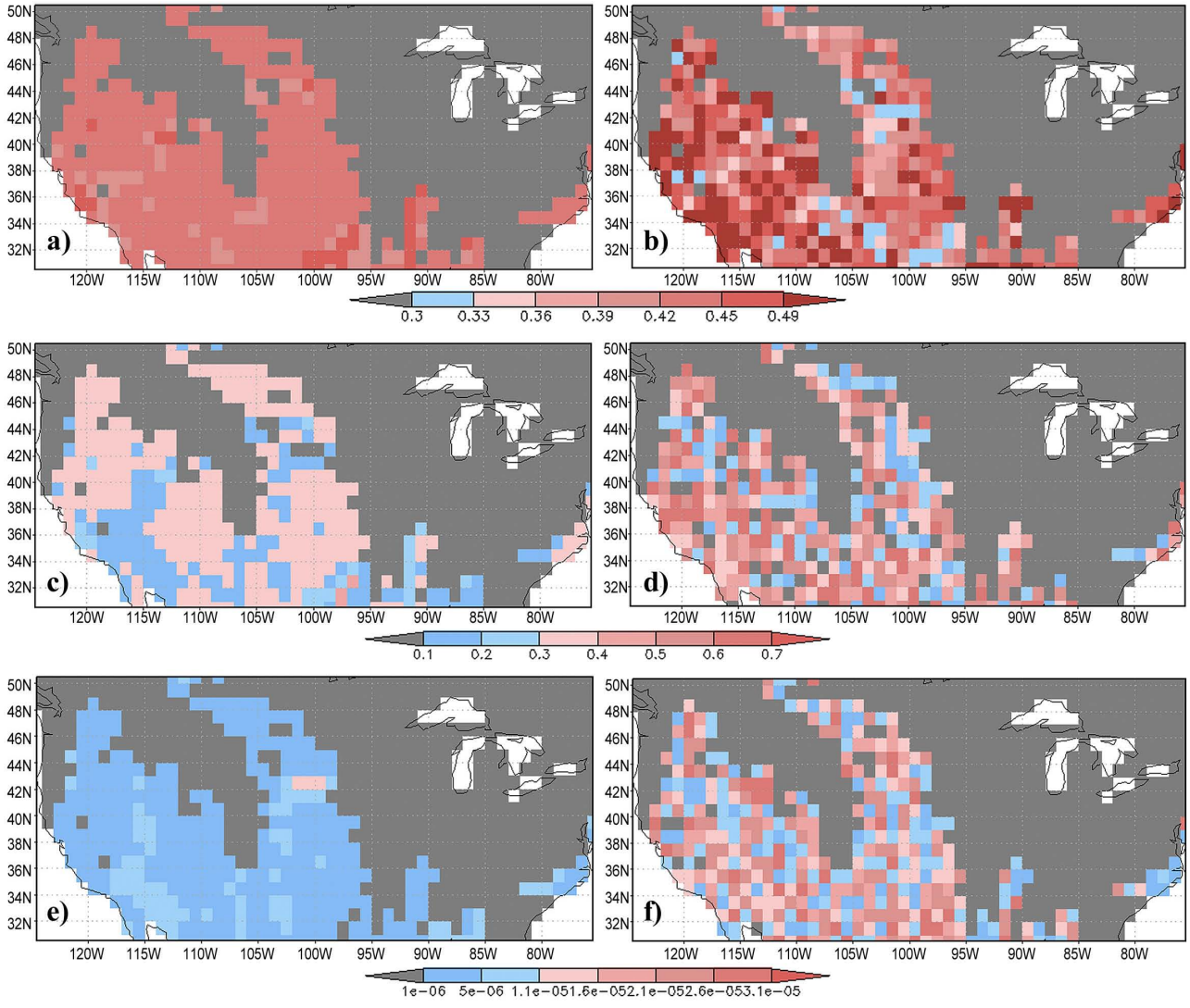

Figure 4. (a, b) Porosity (θ_s, unitless), (c, d) saturated matric potential (ψ_s, unitless), and (e, f) saturated hydraulic conductivity (K_s, in units of m s^{-1}) from (left) look-up tables and (right) estimated through optimization OPT6. The gray color represents grid cells for which parameters were not estimated.

look-up table category-based constraints can be introduced on these parameter ranges to ensure that the estimated parameters conform to the traditional, category-based (e.g., soil texture based) notions of physical realism. Algorithms and approaches that incorporate notions of "equifinal" solutions [e.g., *Gupta et al.*, 1999; *Hogue et al.*, 2006] may offer more effective ways to represent parameter uncertainty and to ensure physical consistency since they generate a range of plausible model fits. The use of such methods is left for a future work. Here the parameter sets generated by the optimization simulations OPT1 and OPT6 may represent mismatches with regard to the typical category-based definitions.

4.2. Data Assimilation Experiments

[36] Section 4.2 presents the results from data assimilation experiments that employ different strategies for bias cor-rection (section 3.2). Since the suite of experiments in-clude simulations that assimilate both unscaled (experiments DA-NOSC, DA-OPT1, and DA-OPT6) and scaled observations (experiments DA-STDN and DA-CDF), we primarily use the anomaly time series correlation coefficient (R), to quantify the skill of the model simulations.

[37] The anomaly time series for each grid point is estimated as follows: The monthly mean climatology values are subtracted from the daily average raw data, so that the anomalies represent the daily deviations from the mean seasonal cycle. The skill contribution from correctly identifying the mean seasonal variation is therefore excluded. The anomaly R values are computed, separately for each grid point, as the correlation coefficients between the daily anomalies from the assimilation estimates and the corresponding truth data. Only anomalies at times and locations for which observations are assimilated contribute to the computation of the R values. Similar to the comparisons in section 4.1, only grid points with at least 600 assimilated observations during the evaluation period are included in the evaluations.

[38] Figure 5 shows the comparison of the anomaly R values for surface soil moisture from different model integrations. Overall, the assimilation experiments perform better than the open loop simulation, and the assimilation skill systematically improves from experiment DA-NOSC to experiment DA-OPT6. The domain-averaged skill of the Noah model integration without any data assimilation (OL) is 0.47. When observations are assimilated without bias correction (DA-NOSC), the domain-averaged skill improves to 0.63. The assimilation skill is further improved in the integrations that employ a priori scaling of observations, with domain-averaged skill values of 0.71 and 0.73 for DA-STDN and DA-CDF, respectively. For the climatological differences encountered in this synthetic experiment, the use of higher-order moments in the CDF matching technique slightly outperforms the seasonally varying scaling parameters used in DA-STDN. Finally, surface soil moisture skill values of 0.73 and 0.75 are obtained for experiments DA-OPT1 and DA-OPT6, respectively, when assimilation integrations are conducted with optimized parameters that conform to the catchment LSM (truth) climatology.

[39] The assimilation of surface soil moisture retrievals is often used as a way to generate superior estimates of related states such as root zone soil moisture [*Reichle et al.*, 2007; *Kumar et al.*, 2009]). Figure 6 presents a comparison of the root zone soil moisture skill estimates from different model integrations. Similar to the behavior observed for surface soil moisture, the skill of root zone estimates from using the calibrated model is comparable to the skills from a priori scaling approaches. The domain-averaged open loop root zone skill estimate is 0.45 and it improves to 0.54 when assimilation is performed without bias correction (DA-NOSC). The skill further improves to 0.62 and 0.63 through the use of a priori scaling of observations for

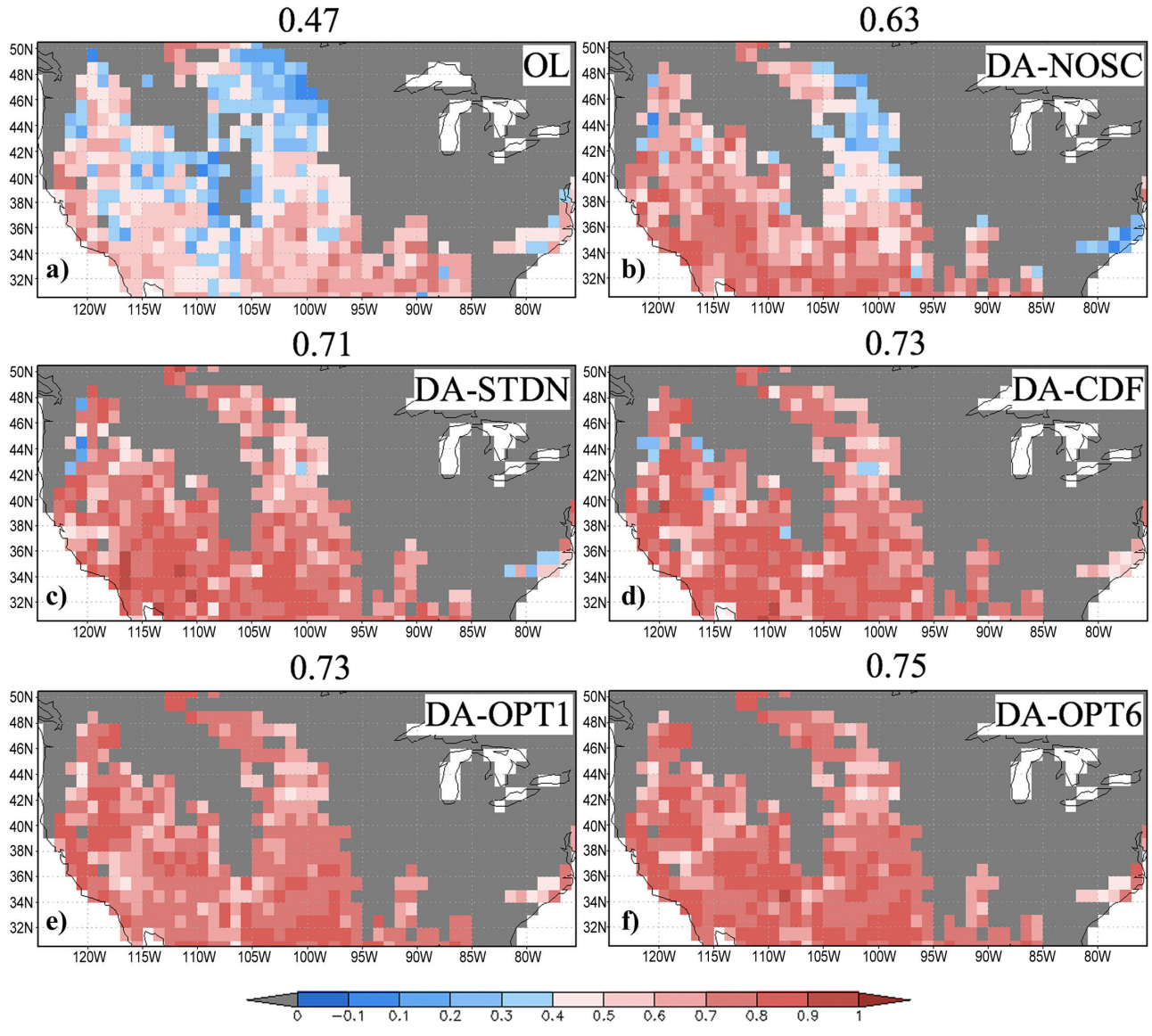

Figure 5. Surface soil moisture skill in terms of anomaly time series correlation coefficients. See Table 2 for definition of experiments. The gray color represents grid cells excluded from the computations. Domain-averaged values are given above each plot.

integrations DA-STDN and DA-CDF, respectively. Finally, the use of a calibrated model together with the assimilation of unscaled observations provides domain-averaged skill values of 0.62 and 0.63 for integrations DA-OPT1 and DA-OPT6, respectively. For root zone soil moisture, the relative advantage of the a priori calibration strategy (DA-OPT1, DA-OPT6) over the a priori scaling methods (DA-STDN, DA-CDF) is minimal. The 95% confidence intervals of the domain-averaged anomaly R values are in the range of 0.008 to 0.01, verifying that the improvements obtained through data assimilation in both surface and root zone soil moisture are statistically significant.

[40] In a separate analysis (not shown), we also examined the skill improvements in surface fluxes (latent, sensible and ground heat) from the data assimilation integrations. The assimilation runs with bias correction (DA-STDN, DA-CDF, DA-OPT1, and DA-OPT6) were found to marginally improve the surface flux skill values over the open loop and DA-NOSC integrations, with a priori scaling and a priori calibration yielding comparable results.

[41] Figures 5 and 6 also indicate that soil moisture skill values improve consistently across the domain in the data assimilation integrations. To further illustrate this fact, Figure 7 shows probability density functions (PDFs) for surface and root zone soil moisture skill values across the modeling domain. Compared to the PDF for the OL integration, the PDFs from data assimilation integrations show narrower distributions that are skewed toward higher skill values because of the improved soil moisture estimates from assimilation. For surface soil moisture, the PDF for DA-NOSC is shifted toward higher R values, but shows only a marginal reduction in the spread compared to the PDF for OL skill (The standard deviation of the PDF reduces from 0.156 to 0.142). The runs based on a priori scaling (DA-STDN and DA-CDF) yield a greater reduction in the OL spread (standard deviation of 0.121 and 0.093, respectively) and a further shift toward higher skill values.

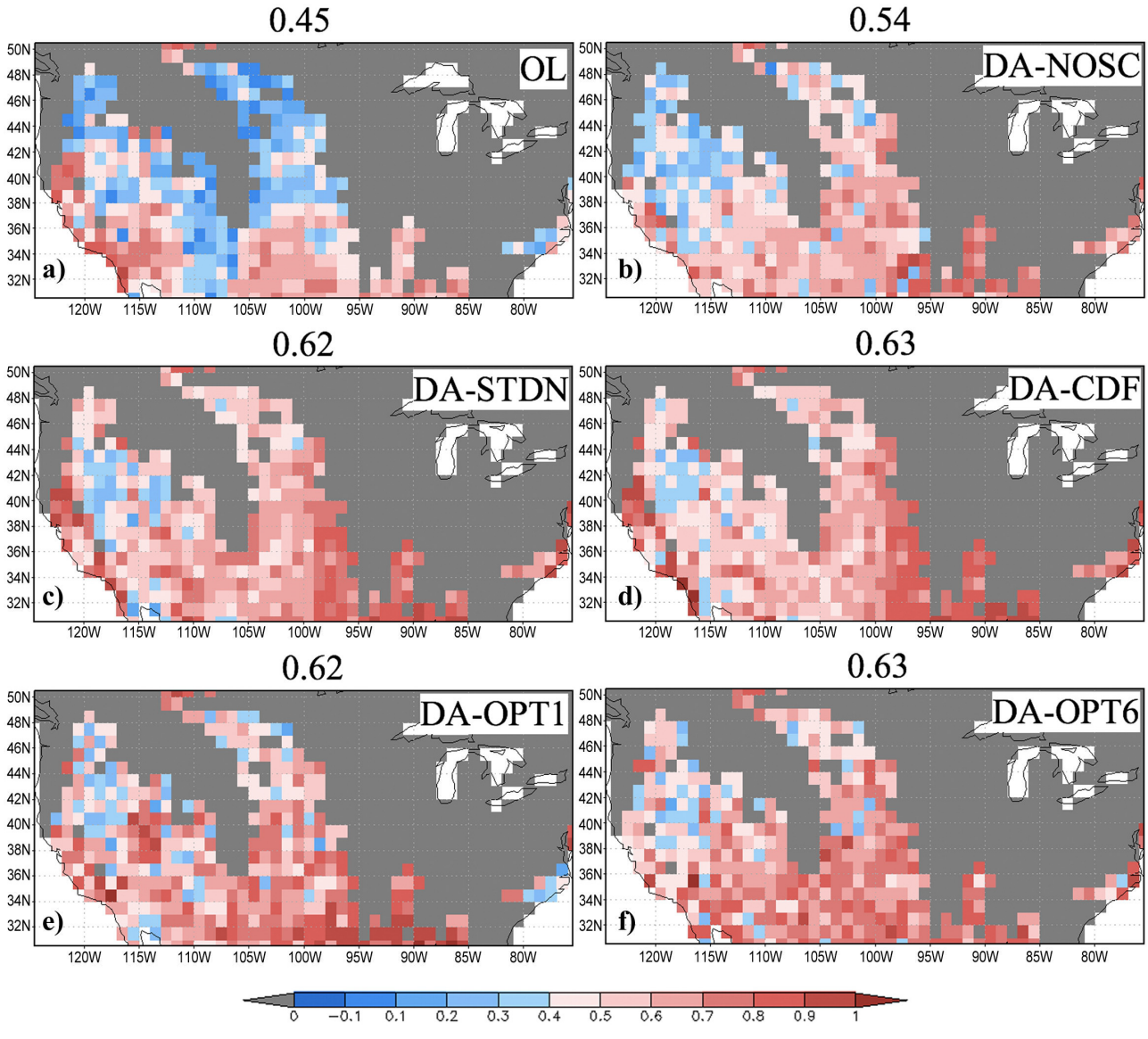

Figure 6. Same as Figure 5, but for root zone soil moisture.

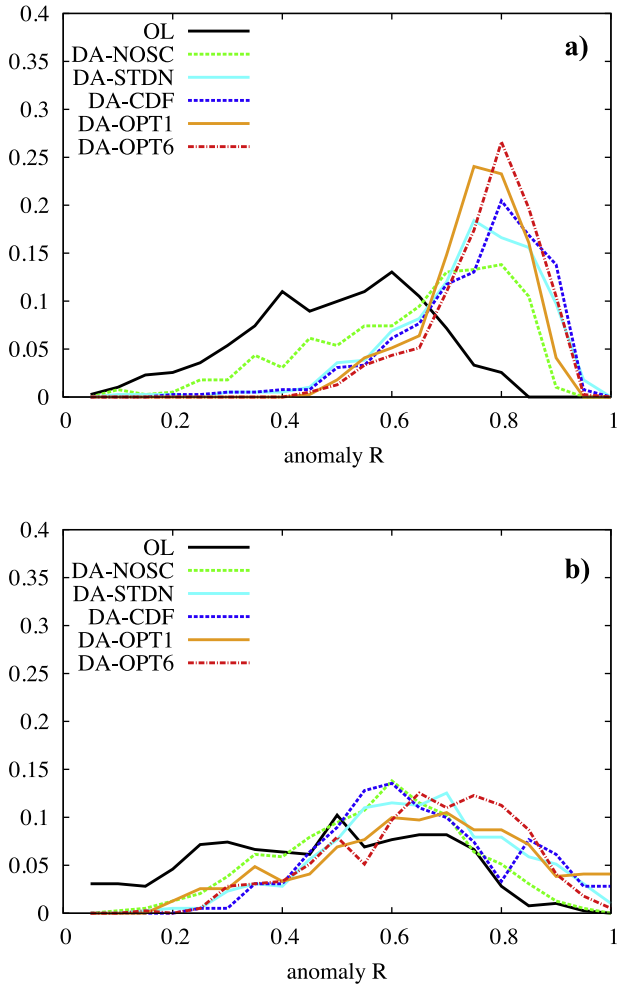

Figure 7. Probability density functions of skill (anomaly R) values across the domain from different model integrations for (a) surface soil moisture and (b) root zone soil moisture.

The DA-OPT1 and DA-OPT6 integrations provide similarly reduced variability in skill estimates (that is, consistent improvements) across the domain with standard deviations in PDFs of 0.113 and 0.091, respectively. Comparable but more muted trends are observed for root zone soil moisture, where the variability in skill values also reduces, gradually from the OL to DA-OPT6. In summary, Figure 7 indicates that a priori calibration and a priori scaling yield comparable improvements in surface and root zone skill.

[42] The anomaly R metric is indifferent to any bias in the mean or the amplitude of variations. By contrast, the RMSE is highly sensitive to biases. As mentioned earlier, the long-term mean bias with respect to the true conditions is difficult (if not impossible) to determine for continental-scale soil moisture. To supplement the anomaly R skill values presented above, we now assess the "unbiased" RMSE (ubRMSE) values, which are computed from the time series after removal of the long-term mean bias [*Entekhabi et al.*, 2010a]. Table 4 provides a comparison of the domain-averaged ubRMSE values from different model simulations, which shows similar trends to those seen with the anomaly R metric. For surface soil moisture, the domain-averaged ubRMSE for the OL integration is 0.052 m^3 m^{-3}, which reduces to 0.041 m^3 m^{-3} for DA-NOSC. The scaling-based DA runs DA-STDN and DA-CDF improve these estimates to 0.038 and 0.037 m^3 m^{-3}, respectively. The optimization-based runs DA-OPT1 and DA-OPT6 provide comparable skills to the scaling-based runs with domain-averaged ubRMSE values of 0.037 and 0.036 m^3 m^{-3}, respectively. The root zone soil moisture skill values follow similar trends. The domain-averaged ubRMSE for OL is 0.039 m^3 m^{-3}, and it improves to 0.037 m^3 m^{-3} in the DA-NOSC simulation. Both a priori scaling- and optimization-based approaches provide systematic, statistically significant improvements (relative to OL) with domain-averaged ubRMSE of 0.035, 0.034, 0.033, and 0.033 m^3 m^{-3} for integrations DA-STDN, DA-CDF, DA-OPT1, and DA-OPT6, respectively.

Table 4. Comparison of Domain-Averaged Unbiased RMSE (ubRMSE) Metric Values From Different Model Integrations[a]

Experiment	Surface Soil Moisture (m^3 m^{-3})	Root Zone Soil Moisture (m^3 m^{-3})
OL	0.052 ± 0.001	0.039 ± 0.001
DA-NOSC	0.041 ± 0.001	0.037 ± 0.001
DA-STDN	0.038 ± 0.001	0.035 ± 0.001
DA-CDF	0.037 ± 0.001	0.034 ± 0.001
DA-OPT1	0.037 ± 0.001	0.033 ± 0.001
DA-OPT6	0.036 ± 0.001	0.033 ± 0.001

[a]All with 95% confidence intervals.

[43] An important aspect of a priori bias mitigation approaches is the fact that they require an a priori estimate of the climatology of the observations. *Reichle and Koster* [2004] demonstrate that for the a priori scaling approach, a single year of observations may be sufficient if some spatial averaging over neighboring grid cells is employed to reduce sampling noise. In this context, it is encouraging that the assimilation skill values from the DA-OPT1 and DA-OPT6 integrations are comparable, with DA-OPT6 generating an additional domain-averaged improvement of only 0.02 over DA-OPT1 for surface and root zone soil moisture. In other words, most of the benefit of the a priori calibration method can be achieved with just 1 year's worth of observations, provided the climatology can be reasonably approximated from the available data year, which is the case here (not shown). This suggests that using a short time period for calibration can still be an effective strategy, which is especially important for new types of satellite missions when the period of available data is relatively short.

[44] Further, note that the objective function formulation (equation (2)) is designed to only correct the first moment of the model and observation distributions, whereas the a priori scaling approaches are designed to correct multiple moments of the distributions. Nevertheless, the assimilation skills from the a priori scaling and a priori optimization approaches are already comparable, indicating that further skill improvements may be achieved using objective function formulations designed to correct multiple moments of the distributions.

4.3. Computational Considerations

[45] Data assimilation with bias mitigation through a priori calibration (DA-OPT1, DA-OPT6) improves surface

and root zone soil moisture estimates compared to bias mitigation through a priori scaling (DA-STDN, DA-CDF). It should be noted, however, that the estimation of the optimization parameters through batch calibration has an associated computational cost. The scalable computing infrastructure in LIS helps in reducing this overhead through parallel computation using multiple processors. The OPT6 integration requires 200 iterations of LIS runs over the 2000–2006 period, which translates to wall clock times of approximately a week, using 128 processors. In comparison, the OPT1 integration requires approximately a day (using 128 processors). The comparable skill of the short calibration-based run (DA-OPT1) relative to the long calibration-based run (DA-OPT6) indicate that the high computational cost associated with batch calibration can be considerably reduced by using a shorter time period of observations that adequately represents the overall climatology. The dimensionality of the decision space can be reduced by selecting a smaller number of parameters that are likely to be more sensitive to the soil moisture simulations. The reduction in the dimensionality of the decision space vector will also aid toward reducing the computational cost associated with optimization simulations.

4.4. Innovation Metrics

[46] In section 4.4, we examine the filter innovations (observation minus model forecast residuals) from the assimilation experiments. This analysis provides insights into the performance of the data assimilation integrations [*Reichle et al.*, 2002; *Crow and Van Loon*, 2006; *Reichle et al.*, 2007; *Kumar et al.*, 2008b]. Strictly speaking, the EnKF provides optimal estimates only if several assumptions hold, including linear system dynamics with model and observation errors that are Gaussian and mutually and serially uncorrelated. If these assumptions hold, then the distribution of normalized innovations (normalized with their expected covariance) follows a standard normal distribution, $N(0,1)$ [*Gelb*, 1974]. The deviations from the expected mean and variance of the normalized innovation distribution provides a measure of the degree of suboptimality with which the assimilation system performs.

[47] Unsurprisingly, the integration without a priori bias mitigation exhibits the largest innovation biases, reflecting strong biases between the (synthetic) observations and the corresponding model forecasts (not shown). The a priori scaling (DA-STDN, DA-CDF) and a priori calibration approaches (DA-OPT1, DA-OPT6) clearly mitigate theses biases (not shown). Figure 8 presents maps of the variance of the normalized innovations. For the bias-blind assimilation integration (DA-NOSC), the variance of the normalized innovations is on average 2.38 and far exceeds the target value of 1, which reflects the strong underestimation of the actual errors by the assimilation system because it ignores the bias. Adding a priori bias mitigation strategies brings the variance of the normalized innovations much closer to the target value of 1. On the basis of this metric, the assimilation using the CDF-based a priori scaling (DA-CDF) operates closer to optimality than the simpler strategy that uses only the first and second order rescaling (DA-STDN). Likewise, variance of the normalized innovations is closer to the target value of 1 when all years are used in the a priori calibration (DA-OPT6) rather than just 1 year (DA-OPT1).

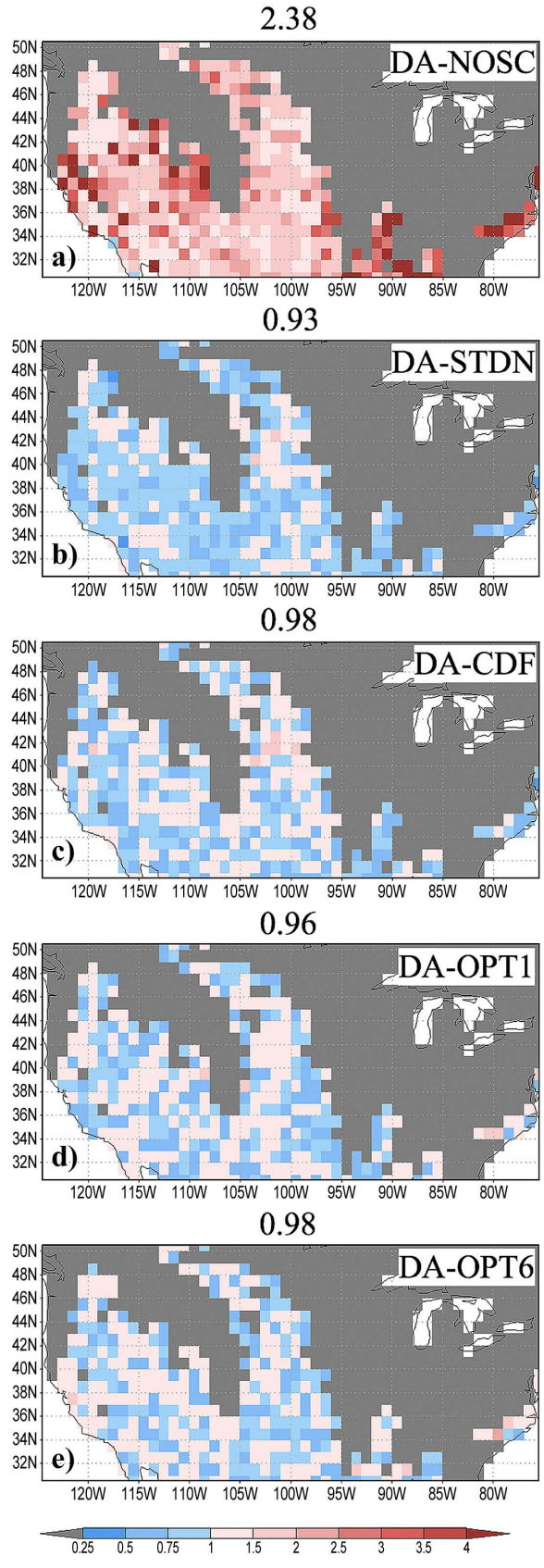

Figure 8. Variance of normalized innovations from different assimilation experiments. The gray color represents grid cells excluded from the computations. Domain-averaged values are given above each plot.

5. Summary

[48] Data assimilation methods such as the EnKF require that the errors in the model and the observations are strictly random. As a result, the presence of systematic or bias errors needs to be addressed separately within the data assimilation system. In this study, we evaluate a number of bias mitigation strategies in the context of assimilating surface soil moisture retrievals. Specifically, we examine the use of land model parameter estimation as a bias correction strategy prior to data assimilation. This strategy is compared to the approach of scaling the assimilated observations to the land model's climatology prior to data assimilation. The study is conducted using a fraternal twin experiment setup, where synthetic observations generated using the catchment LSM are assimilated into the Noah LSM. Five different data assimilation experiments are conducted, each using a different strategy to correct (or not) for bias prior to data assimilation. The resulting soil moisture estimates are evaluated against the corresponding synthetic truth fields from the catchment LSM.

[49] Our results indicate that a priori land model calibration is an effective strategy for bias mitigation in soil moisture assimilation. The domain-averaged skill estimates (in terms of anomaly R values) for the Noah open loop simulation without any data assimilation are 0.47 for surface soil moisture and 0.45 for root zone soil moisture. These skill estimates improve to 0.63 for surface soil moisture and 0.54 for root zone soil moisture. when assimilation is conducted without any bias correction (DA-NOSC). When observations are assimilated after rescaling to the model climatology, the assimilation skill improves further. Two approaches for a priori scaling are considered: (DA-STDN) using standard normal deviates and (DA-CDF) by matching the CDFs of the observations to that of the model. Assimilation using these a priori scaling approaches yields domain-averaged skill values of 0.71 and 0.73 for surface soil moisture and 0.62 and 0.63 for root zone soil moisture, respectively. Similar improvements in the surface and root zone soil moisture estimates are observed with the assimilation runs that employ optimized model parameters but ingest unscaled observations. Two sets of optimized parameters are used in the experiments: (DA-OPT1) parameters estimated from a single year of calibration and (DA-OPT6) parameters estimated from 6 years of calibration. When data assimilation is conducted using parameters from a single year of calibration, skill estimates of 0.73 for surface soil moisture and 0.62 for root zone soil moisture are obtained. The use of the 6 year based parameters further improves these skill measures to 0.75 for surface soil moisture and 0.63 for root zone soil moisture.

[50] It was also observed that spatial variability in the skill scores across the domain is reduced with the use of optimized parameters, resulting in more spatially consistent skill enhancements. The skill improvements in surface fluxes were found to be comparable for data assimilation following a priori scaling and a priori calibration. Similar trends in skill scores are also observed if the unbiased RMSE metric is used instead of anomaly R for evaluating the results. Finally, the analysis of innovation diagnostics also demonstrates that without the use of suitable bias correction, the assimilation system performs in a less than optimal manner and that all four bias mitigation strategies adequately address the bias issue.

[51] In the suite of synthetic experiments presented in this article we are in effect calibrating the Noah surface soil moisture climatology to that of the catchment LSM. It must be stressed that this approach is chosen not because one model (catchment) is more correct than the other (Noah). A similar argument holds when satellite soil moisture retrievals are assimilated. In that case, the climatology of the retrievals is not necessarily more correct than that of the model. However, when brightness temperatures are assimilated in radiance space instead of the retrievals, the model should be calibrated to the observed brightness temperature climatology. The long-term biases can be mitigated through calibration and the remaining shorter-term biases can be addressed with a priori scaling. The combined use of these strategies will be examined in future radiance-based data assimilation experiments.

[52] Though effective, the approach of using parameter estimation for bias correction also suffers from the limitations of the a priori scaling approaches. Since the parameters are estimated in advance of data assimilation, any subsequent changes in model behavior will not be captured, unlike in the dynamic bias estimation algorithms. The optimization formulation does not constrain the estimated parameters to conform to the traditional, look-up table–based definitions of parameters. Here no attempt was made to ensure the physical realism of the estimated parameters. The calibration might also require additional constraints to ensure that the behavior of related variables is not adversely affected. Note, however, that we have found that the estimates of the latent and sensible heat fluxes were comparable for the assimilation integrations with bias correction (DA-STDN, DA-CDF, DA-OPT1, and DA-OPT6). Furthermore, our results suggest that using model parameter estimation could be a viable strategy for bias mitigation in cases of relatively short (i.e., 1 year) satellite records. This result is important for expediting the use of soil moisture retrievals becoming available from SMOS and SMAP.

[53] The study also demonstrates the advanced capabilities of the NASA LIS framework, including the development of a new subsystem for optimization. This extension encapsulates a range of advanced search algorithms suited for both convex and nonconvex optimization problems. In this particular study, the genetic algorithm, a heuristic search technique based on principles of evolutionary computing, is employed for estimating model parameters. The optimization infrastructure within LIS is currently being enhanced with a suite of uncertainty estimation algorithms based on Bayesian methods. In contrast to the optimization techniques that have already been implemented in LIS and generate a single solution for parameters, the newer uncertainty estimation tools infer distributions of parameters based on the observational information. These parameter distributions can then be used to condition the ensembles used in the data assimilation system. The joint use of optimization and data assimilation tools presented here and future LIS advancements will enable the increased exploitation of observational data for improving hydrological modeling.

[54] **Acknowledgments.** We gratefully acknowledge the financial support from the NASA Earth Science Technology Office (ESTO) (Advanced

Information System Technology program award AIST-08-077). Rolf Reichle was supported by the NASA program on Earth System Science Research using Data and Products from Terra, Aqua, and ACRIMSAT satellites and the SMAP Science Definition Team. We thank James Geiger, Scott Rheingrover, and Dalia Kirschbaum for helpful comments. Computing was supported by the resources at the NASA Center for Climate Simulation.

References

Bosilovich, M., J. Radakovich, A. da Silva, R. Todling, and F. Verter (2007), Skin temperature analysis and bias correction in a coupled land-atmosphere data assimilation system, *J. Meteorol. Soc. Jpn.*, *85A*, 205–228.

Boulet, G., Y. Kerr, and A. Chehbouni (2002), Deriving catchment-scale water and energy balance parameters using data assimilation based on extended Kalman filtering, *Hydrol. Sci. J. Sci. Hydrol.*, *47*, 449–467.

Braun, F., and G. Schadler (2005), Comparison of soil hydraulic parameterizations for mesoscale and meteorological models, *J. Appl. Meteorol.*, *44*, 1116–1132.

Burke, E., R. Gurney, L. Simmonds, and T. Jackson (1997), Calibrating a soil water and energy budget with remotely sensed data to obtain quantitative information about the soil, *Water Resour. Res.*, *33*, 1689–1697.

Cosby, B., G. Hornberger, R. Clapp, and T. Ginn (1984), A statistical exploration of the relationships of soil moisture characteristics to the physical properties of soils, *Water Resour. Res.*, *20*, 682–690.

Crow, W. T., and E. Van Loon (2006), Impact of incorrect model error assumptions on the sequential assimilation of remotely sensed surface soil moisture, *J. Hydrometeorol.*, *7*, 421–432.

Crow, W., R. Koster, R. Reichle, and H. Sharif (2005), Relevance of time-varying and time-invariant retrieval error sources on the utility of spaceborne soil moisture products, *Geophys. Res. Lett.*, *32*, L24405, doi:10.1029/2005GL024889.

DeChant, C., and H. Moradkhani (2011), Radiance data assimilation for operational snow and streamflow forecasting using the particle filter, *Adv. Water Resour.*, *34*, 351–364.

Dee, D. (2005), Bias and data assimilation, *Q. J. R. Meteorol. Soc.*, *131*, 3323–3343.

Dee, D., and A. da Silva (1998), Data assimilation in the presence of forecast bias, *Q. J. R. Meteorol. Soc.*, *124*, 269–295.

De Lannoy, G., P. Houser, V. Pauwels, and N. Verhoest (2007a), State and bias estimation for soil moisture profiles by an ensemble Kalman filter: Effect of assimilation depth and frequency, *Water Resour. Res.*, *43*, W06401, doi:10.1029/2006WR005100.

De Lannoy, G., R. Reichle, P. Houser, V. Pauwels, and N. Verhoest (2007b), Correcting for forecast bias in soil moisture assimilation with the ensemble Kalman filter, *Water Resour. Res.*, *43*, W09410, doi:10.1029/2006WR005449.

Derber, J., D. Parrish, and S. Lord (1991), The new global operational analysis system at the National Meteorological Center, *Weather Forecast.*, *6*, 538–547.

Doherty, J., and D. Welter (2010), A short explanation of structural noise, *Water Resour. Res.*, *46*, W05525, doi:10.1029/2009WR008377.

Draper, C., J. Mahfouf, and J. Walker (2009), An EKF assimilation of AMSR-E soil moisture into the ISBA land surface scheme, *J. Geophys. Res.*, *114*, D20104, doi:10.1029/2008JD011650.

Draper, C., J. Mahfouf, and J. Walker (2011), Root zone soil moisture from the assimilation of screen-level variables and remotely sensed soil moisture, *J. Geophys. Res.*, *116*, D02127, doi:10.1029/2010JD013829.

Drusch, M., E. Wood, and H. Gao (2005), Observation operators for the direct assimilation of TRMM microwave imager retrieved soil moisture, *Geophys. Res. Lett.*, *32*, L15403, doi:10.1029/2005GL023623.

Duan, Q., S. Sorooshian, and V. Gupta (1992), Effective and efficient global optimization for conceptual rainfall-runoff models, *Water Resour. Res.*, *28*, 1015–1031.

Duan, Q., V. Gupta, and S. Sorooshian (1993), A shuffled complex evolution approach for effective and efficient global minimization, *J. Optim. Theory. Appl.*, *76*, 501–521.

Ek, M., K. Mitchell, L. Yin, P. Rogers, P. Grunmann, V. Koren, G. Gayno, and J. Tarpley (2003), Implementation of Noah land-surface model advances in the NCEP operational mesoscale Eta model, *J. Geophys. Res.*, *108*(D22), 8851, doi:10.1029/2002JD003296.

Entekhabi, D., R. Reichle, R. Koster, and W. Crow (2010a), Performance metrics for soil moisture retrievals and application requirements, *J. Hydrometeorol.*, *11*, 832–840.

Entekhabi, D., et al. (2010b), The Soil Moisture Active Passive (SMAP) Mission, *Proc. IEEE*, *98*, 704–716, doi:10.1109/JPROC.2010.2043918.

Gelb, A. (1974), *Applied Optimal Estimation*, MIT Press, Cambridge, Mass.

Goldberg, D. (1989), *Genetic Algorithms in Search, Optimization and Machine Learning*, Addison-Wesley, Reading, Mass.

Gupta, H., L. Bastidas, S. Sorooshian, W. Shuttleworth, and Z. Yang (1999), Parameter estimation of a land surface scheme using multicriteria methods, *J. Geophys. Res.*, *104*, 19,491–19,503.

Gutman, E., and E. Small (2010), A method for the determination of the hydraulic properties of soil from MODIS surface temperature for use in land surface models, *Water Resour. Res.*, *46*, W06520, doi:10.1029/2009WR008203.

Hill, C., C. DeLuca, V. Balaji, M. Suarez, and A. da Silva (2004), A architecture of the Earth system modeling framework, *Comput. Sci. Eng.*, *6*(1), 18–28.

Hogue, T., L. Bastidas, H. Gupta, S. Sorooshian, K. Mitchell, and W. Emmerich (2005), Evaluation and transferability of the Noah land surface model in semiarid environments, *J. Hydrometeorol.*, *6*, 68–84.

Hogue, T. S., L. A. Bastidas, H. V. Gupta, and S. Sorooshian (2006), Evaluating model performance and parameter behavior for varying levels of land surface model complexity, *Water Resour. Res.*, *42*, W08430, doi:10.1029/2005WR004440.

Holland, J. (1975), *Adaptation in Natural and Artificial Systems*, Univ. of Mich. Press, Ann Arbor.

Kerr, Y. H., et al. (2010), The SMOS mission: New tool for monitoring key elements of the global water cycle, *Proc. IEEE*, *98*, 666–687.

Koster, R. D., M. J. Suarez, A. Ducharne, M. Stieglitz, and P. Kumar (2000), A catchment-based approach to modeling land surface processes in a general circulation model: 1. Model structure, *J. Geophys. Res.*, *105*, 24,809–24,822.

Kumar, S., et al. (2006), Land information system: An interoperable framework for high resolution land surface modeling, *Environ. Model. Software*, *21*, 1402–1415.

Kumar, S., C. Peters-Lidard, Y. Tian, R. H. Reichle, C. Alonge, J. Geiger, J. Eylander, and P. Houser (2008a), An integrated hydrologic modeling and data assimilation framework enabled by the Land Information System (LIS), *IEEE Comput.*, *41*, 52–59.

Kumar, S., R. Reichle, C. Peters-Lidard, R. Koster, X. Zhan, W. Crow, J. Eylander, and P. Houser (2008b), A land surface data assimilation framework using the Land Information System: Description and applications, *Adv. Water Resour.*, *31*, 1419–1432, doi:10.1016/j.advwatres.2008.01.013.

Kumar, S. V., R. H. Reichle, R. D. Koster, W. T. Crow, and C. D. Peters-Lidard (2009), Role of subsurface physics in the assimilation of surface soil moisture observations, *J. Hydrometeorol.*, *11*, 1103–1122, doi:10.1175/2010JHM1262.1.

Lambot, S., E. Slob, J. Rhebergen, O. Lopera, K. Jadoon, and H. Vereecken (2009), Remote estimation of the hydraulic properties of a sand using full-waveform integrated hydrogeophysical inversion of time-lapse, off-ground GPR data, *Vadose Zone J.*, *8*, 743–754.

Levenberg, K. (1944), A method for the solution of certain non-linear problems in least squares, *Q. Appl. Math.*, *2*, 164–168.

Liu, Q., R. H. Reichle, R. Bindlish, M. H. Cosh, W. T. Crow, R. de Jeu, G. J. M. De Lannoy, G. J. Huffman, and T. J. Jackson (2011), The contributions of precipitation and soil moisture observations to the skill of soil moisture estimates in a land data assimilation system, *J. Hydrometeorol.*, *12*, 750–765, doi:10.1175/JHM-D-10-05000.1.

Liu, Y., and H. Gupta (2007), Uncertainty in hydrologic modeling: Toward an integrated data assimilation framework, *Water Resour. Res.*, *43*, W07401, doi:10.1029/2006WR005756.

Liu, Y., H. Gupta, S. Sorooshian, L. Bastidas, and W. Shuttleworth (2004), Exploring parameter sensitivities of the land surface using a locally coupled land-atmosphere model, *J. Geophys. Res.*, *109*, D21101, doi:10.1029/2004JD004730.

Liu, Y., H. Gupta, S. Sorooshian, L. Bastidas, and W. Shuttleworth (2005), Constraining land surface and atmospheric parameters of a locally coupled model using observational data, *J. Hydrometeorol.*, *6*, 156–172.

Mahrt, L., and H. Pan (1984), A two-layer model of soil hydrology, *Boundary Layer Meteorol.*, *29*, 1–20.

Marquardt, D. (1963), An algorithm for least-squares estimation of non-linear parameters, *SIAM J. Appl. Math.*, *11*, 431–441.

Montzka, C., H. Moradkhani, L. Weihermuller, M. Canty, H. Hendricks Frassen, and H. Vereecken (2011), Hydraulic parameter estimation by remotely-sensed top soil moisture observations with the particle filter, *J. Hydrol.*, *399*, 410–421.

Moradkhani, H., K.-L. Hsu, H. Gupta, and S. Sorooshian (2005a), Uncertainty assessment of hydrologic model states and parameters: Sequential

data assimilation using the particle filter, *Water Resour. Res.*, *41*, W05012, doi:10.1029/2004WR003604.

Moradkhani, H., S. Sorooshian, H. Gupta, and P. Houser (2005b), Dual state-parameter estimation of hydrological models using ensemble Kalman filter, *Adv. Water Resour.*, *28*, 135–147.

Nearing, G., M. Moran, K. Thorp, C. Collins, and D. Slack (2010), Likelihood parameter estimation for calibrating a soil moisture model using radar backscatter, *Remote Sens. Environ.*, *114*, 2564–2574.

Nie, S., J. Zhu, and Y. Luo (2011), Simultaneous estimation of land surface scheme states and parameters using the ensemble Kalman filter: Identical twin experiments, *Hydrol. Earth Syst. Sci.*, *15*, 2437–2457.

Peters-Lidard, C. D., et al. (2007), High-performance Earth system modeling with NASA/GSFC's land information system, *Innovations Syst. Software Eng.*, *3*, 157–165.

Peters-Lidard, C., D. Mocko, M. Garcia, J. Santanello, M. Tischler, and M. Moran (2008), Role of precipitation uncertainty in the estimation of hydrologic soil properties using remotely sensed soil moisture in a semiarid environment, *Water Resour. Res.*, *44*, W05S18, doi:10.1029/2007WR005884.

Qin, J., S. Liang, K. Yang, I. Kaihotsu, R. Liu, and T. Koike (2009), Simultaneous estimation of both soil moisture and model parameters using particle filtering method through the assimilation of microwave signal, *J. Geophys. Res.*, *114*, D15103, doi:10.1029/2008JD011358.

Rawls, W., D. Brakensiek, and K. Saxton (1982), Estimation of soil water properties, *Trans. ASAE*, *25*, 1316–1320.

Reichle, R., and R. Koster (2003), Assessing the impact of horizontal error correlations in background fields on soil moisture estimation, *J. Hydrometeorol.*, *4*, 1229–1242.

Reichle, R. H., and R. Koster (2004), Bias reduction in short records of satellite soil moisture, *Geophys. Res. Lett.*, *31*, L19501, doi:10.1029/2004GL020938.

Reichle, R., D. McLaughlin, and D. Entekhabi (2002), Hydrologic data assimilation with the ensemble Kalman filter, *Mon. Weather Rev.*, *130*, 103–114.

Reichle, R., R. Koster, J. Dong, and A. Berg (2004), Global soil moisture from satellite observations, land surface models, and ground data: Implications for data assimilation, *J. Hydrometeorol.*, *5*, 430–442.

Reichle, R., R. Koster, S. Liu, S. P. P. Mahanama, E. Njoku, and M. Owe (2007), Comparison and assimilation of global soil moisture retrievals from the Advanced Microwave Scanning Radiometer for the Earth Observing System (AMSR-E) and the Scanning Multichannel Microwave Radiometer (SMMR), *J. Geophys. Res.*, *112*, D09108, doi:10.1029/2006JD008033.

Reichle, R., M. Bosilovich, W. Crow, R. Koster, S. Kumar, S. Mahanama, and B. Zaitchick (2009), Recent advances in land data assimilation at the NASA Global Modeling and Assimilation Office, in *Data Assimilation for Atmospheric, Oceanic and Hydrologic Applications*, edited by S. K. Park and L. Xu, pp. 407–428, Springer, Berlin.

Reichle, R. H., S. V. Kumar, S. P. P. Mahanama, R. D. Koster, and Q. Liu (2010), Assimilation of satellite-derived skin temperature observations into land surface models, *J. Hydrometeorol.*, *11*, 1103–1122, doi:10.1175/2010JHM1262.1.

Santanello, J., C. Peters-Lidard, M. Garcia, D. Mocko, M. Tischler, M. Moran, and D. Thoma (2007), Using remotely sensed estimates of soil moisture to infer spatially distributed soil hydraulic properties, *Remote Sens. Environ.*, *110*, 79–97.

Schaap, M. (2004), Accuracy and uncertainty in PTF predictions, in *Developments in Soil Science*, edited by Y. Pachepsky and W. J. Rawls, vol. 30, 33–43 pp., Elsevier, Amsterdam, doi:10.1016/S0166-2481(04)30003-6, ISBN 9780444517050.

Slater, A., and M. Clark (2006), Snow data assimilation via an ensemble Kalman filter, *J. Hydrometeorol.*, *7*, 478–493.

Trigo, I., and P. Viterbo (2003), Clear-sky window channel radiances: A comparison between observations and the ECMWF model, *J. Appl. Meteorol.*, *42*, 1463–1479.

Vrugt, J., C. Diks, H. Gupta, W. Bouten, and J. Verstaten (2005), Improved treatment of uncertainty in hydrologic modeling: Combining the strengths of global optimization and data assimilation, *Water Resour. Res.*, *41*, W01017, doi:10.1029/2004WR003059.

Yang, K., T. Koike, I. Kaihotsu, and J. Qin (2009), Validation of a dual-pass microwave land data assimilation system for estimating surface soil moisture in semiarid regions, *J. Hydrometeorol.*, *10*, 780–793.

K. W. Harrison and S. Yatheendradas, Earth System Science Interdisciplinary Center, 5825 University Research Ct., Suite 4001, College Park, MD 20742, USA.

S. V. Kumar, C. D. Peters-Lidard, and J. A. Santanello, Hydrological Sciences Laboratory, NASA Goddard Space Flight Center, Code 617, Greenbelt, MD 20771, USA. (sujay.v.kumar@nasa.gov)

R. H. Reichle, Global Modeling and Assimilation Office, NASA Goddard Space Flight Center, Code 610.1, Greenbelt, MD 20771, USA.